# UNDRAINED BEARING CAPACITY OF A SKIRTED STRIP FOUNDATION USING UPPER-BOUND LIMIT ANALYSIS

# NOSILNOST PASOVNIH TEMELJEV S KRILI V NEDRENIRANIH POGOJIH S POMOČJO ANALIZE ZGORNJE MEJNE VREDNOSTI

**Priyanka Ghosh** *(corresponding author)*
Indian Institute of Technology, Kanpur,
Department of Civil Engineering
Kanpur – 208 016, India
E-mail: priyog@iitk.ac.in

**Alok Pal**
Indian Institute of Technology, Kanpur,
Department of Civil Engineering
Kanpur – 208 016, India
E-mail: alok.besu2188@gmail.com

DOI https://doi.org/10.18690/actageotechslov.16.2.2-11.2019

**Keywords**

footings, limit analysis, plane strain, plasticity, skirted foundation

**Ključne besede**

temelji, mejna analiza, ravninsko deformacijski stanje, plastičnost, temelj s krili

**Abstract**

*Skirted foundations are assumed to be a wise selection in offshore geotechnical engineering. In this paper the bearing-capacity factors for a vertically loaded skirted strip foundation resting on uniform c-ϕ soil were obtained using an upper-bound limit analysis. The analysis is performed by choosing a kinematically admissible failure mechanism comprising multiple triangular rigid blocks. The effect of the embedment depth of the skirts on the bearing capacity is studied based on the dimensionless embedment ratio $D_f/B_f$. A detailed parametric study is carried out by varying the $D_f/B_f$ ratio and ϕ for both the smooth and rough surface of the skirts. The results obtained from the present theoretical analysis are compared with the available theoretical and experimental data reported in the literature.*

**Izvleček**

*V geotehničnem inženirstvu na morju so temelji s krili praviloma primeren izbor temeljenja. V tem prispevku smo s pomočjo analize zgornje mejne vrednosti določili faktorje nosilnosti za vertikalno obremenjen pasovni temelj na enakomerni c-ϕ zemljini. Analiza je izvedena z izbiro kinematično dopustnega porušnega mehanizma, ki je sestavljen iz več trikotnih togih blokov. Vpliv globine vpetja kril na nosilnost je preučevana na podlagi brezdimenzijskega razmerja vpetosti, $D_f/B_f$. Izvedena je bila podrobna parametrična študija s spreminjanjem razmerja $D_f/B_f$ in ϕ za gladko in grobo površino kril. Rezultati, dobljeni na osnovi predlagane teoretične analize, so bili primerjani z razpoložljivimi teoretičnimi in eksperimentalnimi podatki, ki so navedeni v literaturi.*

List of symbols:

| | |
|---|---|
| $B_f$ | width of the skirted strip foundation |
| $D_f$ | embedment depth of the skirts |
| $D_f/B_f$ | non-dimensional embedment ratio |
| $N_{csk}$ | bearing-capacity factor for an isolated skirted strip foundation with respect to the cohesion of the soil |
| $N_\gamma$ | bearing-capacity factor for surface strip foundation with respect to the unit weight of the soil |
| $N_{\gamma sk}$ | bearing-capacity factor for an isolated skirted strip foundation with respect to the unit weight of the soil |
| $P_{usk}$ | ultimate failure load of the skirted foundation |
| $V_i$ | absolute velocity of the $i^{th}$ triangular rigid block in the radial shear zone of the skirted foundation |

| | |
|---|---|
| $V_{i,i+1}$ | velocity of the block $i$+1 relative to the block i in the radial shear zone of the skirted foundation |
| $l_i$, $d_i$ | length of two arms of the $i^{th}$ triangular rigid block in the radial shear zone of the skirted foundation |
| $n$ | number of triangular rigid blocks in the radial shear zone of the skirted foundation |
| $q_{usk}$ | ultimate bearing capacity of the skirted foundation |
| $\alpha_i$, $\beta_i$ | internal angles of the $i^{th}$ triangular rigid block in the radial shear zone of the skirted foundation |
| $\alpha^a$ | adhesion factor for the soil |
| $\phi$ | angle of internal friction of the soil |

## 1 INTRODUCTION

To improve the bearing-capacity and reduce settlement, skirted foundations are reported as a popular choice in geotechnical engineering. The skirts provide confinement in which the soil is stringently enclosed and perform as a single unit with the overlain foundation to transmit the superstructure load to the soil essentially at the level of the skirt tip. Skirted foundations are generally installed to increase the effective depth of the offshore foundation where scouring seems, by all accounts, to be a noteworthy concern [1-4]. Besides that, for several coastal and near-shore structures resting on granular soils with high water tables as well as for the enhancement of the bearing capacity under normal situations, skirted foundations can be an economical option. The major application of skirted foundations is affiliated with jack-up unit structures, oil and petrol gas plants, tension leg platforms, wind-turbine foundations, bridge foundations, etc. Several studies [2-21] are available to determine the bearing capacity of the skirted foundation assuming a rigid soil plug within the skirts. Having considered an equivalent embedded rigid foundation, Yun and Bransby [21] determined the bearing capacity of the skirted foundation embedded in uniform soil. The soil plug is generally presumed to act as a rigid body with uniform shear strength along the depth [14]. Keawsawasvong and Ukritchon [2] and Ukritchon and Keawsawasvong [3] determined the undrained pullout capacity of suction caissons using both upper- and lower-bound limit analyses. A number of investigations [22-28] reported in the literature address the bearing-capacity aspect of the foundation under different field conditions using various solution techniques, such as upper- and lower-bound limit analyses, and finite-element analysis. However, the few studies [13, 21] available in the literature are restricted to the experimental investigation of the skirted foundation considering the plane-strain condition and a perfectly rough foundation-soil interface. Finite-element analyses were performed by Mana et al. [14] to determine the bearing capacity of a circular skirted foundation as a function of the skirt depth, the foundation-soil interface roughness and the heterogeneity in soil strength. However, except for a few studies on suction caissons [2-4], no work is available in the literature to understand the failure of the skirted foundation through a kinematically admissible collapse mechanism along with a properly defined velocity field under the framework of a limit analysis. Therefore, there is an obvious need to develop a proper failure mechanism for exploring the bearing capacity of a skirted foundation theoretically.

This study aims to determine the bearing capacity of a skirted strip foundation resting on a homogeneous soil deposit using upper-bound limit analysis [2-3, 22]. The upper-bound theorem, which assumes a perfectly plastic soil model with an associated flow rule, states that the rate of internal energy dissipation by any kinematically admissible velocity field can be equated with the rate of work done by external forces to enable a strict upper bound on the true limit load [29]. In association with the collapse mechanism similar to Pal et al. [17], a multi-block failure mechanism along with upper-bound limit analysis has been adopted to determine the bearing-capacity factors. The bearing-capacity factors with respect to the cohesion ($N_{csk}$) and unit weight ($N_{ysk}$) of the soil are obtained using a kinematically admissible velocity field. Both smooth and rough skirts are considered in the analysis. The effect of the skirt depth on the bearing capacity is studied based on the dimensionless embedment ratio. The results obtained from the analysis are suitably compared with the available data reported in the literature.

## 2 PROBLEM DEFINITION

A single, isolated, skirted strip foundation with width $B_f$ and depth of skirts $D_f$ rests on a uniform $c$-$\phi$ soil deposit. The objective is to determine the bearing-capacity factors $N_{csk}$ and $N_{ysk}$ considering an upper-bound limit analysis along with a multi-block failure mechanism. The collapse mechanism, as shown in Fig. 1, is supposed to determine the bearing-capacity factors for the skirted foundation. It is assumed: 1) foundation, skirt and connection between the foundation and the skirt behave as a rigid structure; 2) the analysis does not consider the effect of the installation of the skirted foundation on the surrounding soil; 3) the behavior of the soil is considered to be pressure independent, i.e., the undrained condition.

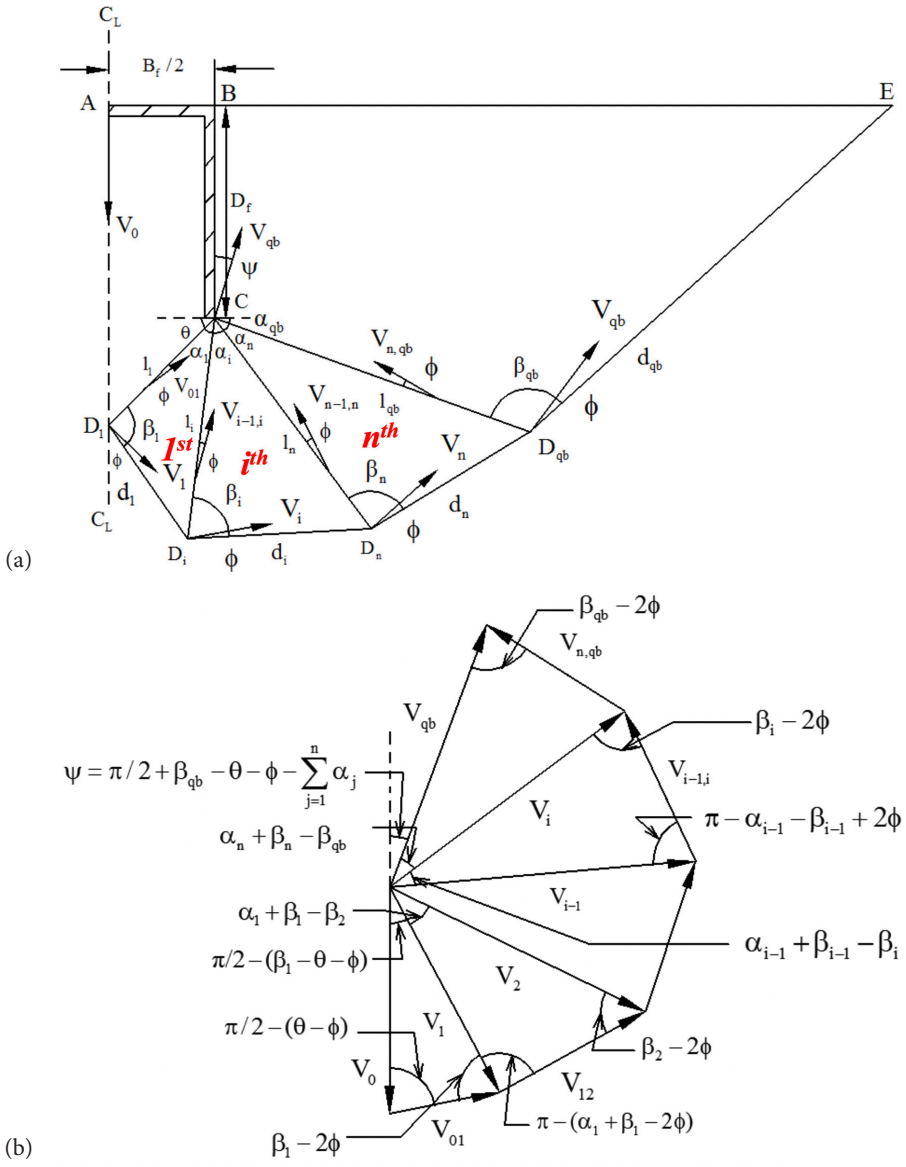


**Figure 1**. (a) Geometry of rigid blocks and velocity vectors, (b) velocity hodograph for failure mechanism.

## 3 FAILURE MECHANISM

The collapse mechanism, as shown in Fig. 1a, is a kinematically admissible, symmetrical, multi-block failure mechanism with three kinematic variables ($\alpha_i$, $\beta_i$ and $\theta$) to define the collapse mechanism. For the sake of clarity, only the right portion of the center line of the foundation is shown in Fig. 1a, where AB and BC are the half width of the foundation and the right skirt, respectively. The wedge $ABCD_1$ is assumed to move vertically as a rigid body with the same downward velocity $V_0$ as that of the footing. The downward movement of the footing and the wedge $ABCD_1$ is accommodated by a lateral movement of the adjacent two radial shear zones on both the left and right sides. The radial shear zones on the right side $CD_1D_2\ldots D_i\ldots D_nD_{qb}C$ are discretized into $n$ number of triangular rigid blocks along with the last quadrilateral rigid block $BCD_{qb}E$. The wedge $ABCD_1$ includes a part of the soil plug formed between two skirts (left and right) and the triangular wedge shaped below the skirts, which makes an angle $\theta$ with the horizontal. Each triangular rigid block within the radial shear zone can be defined by the internal angles $\alpha_i$ and $\beta_i$, and by two arms $l_i$ and $d_i$, whereas the last quadrilat-

eral rigid block, $BCD_{qb}E$ can be defined by the angles $(\pi/2 + \alpha_{qb})$ and $\beta_{qb}$, and the arm length $l_{qb}$, where $l_{qb} = CD_{qb}$. The velocity hodograph for the failure mechanism and other associated geometric parameters are shown in Fig. 1b.

At collapse, it is assumed that the footing and the underlying rigid block $ABCD_1$ move as a single rigid unit in the vertical direction with a velocity $V_0$. The number ($n$) of triangular rigid blocks is kept equal to 30 based on the convergence study. $V_1, V_2, \ldots V_i \ldots V_n$ are the absolute velocities of all the triangular rigid blocks within the radial shear zone, whereas $V_{01}$ is the velocity of the block $CD_1D_2$ relative to the block $ABCD_1$; $V_{i,i+1}$ is the velocity of the block $i$+1 relative to the block $i$ and so on. The interfaces of all the triangular blocks are treated as the velocity-discontinuity lines. The soil mass is assumed to obey the Mohr–Coulomb failure criterion and an associated flow rule. Hence, the direction of the velocity vectors $V_1, V_2, \ldots V_i \ldots V_n$ makes an angle $\phi$ with the corresponding rupture lines. The relative velocities $V_{01}, V_{12}, \ldots V_{i-1,i} \ldots V_{n-1,n}$ are also inclined at an angle $\phi$ with the velocity discontinuity lines $CD_1, CD_2 \ldots CD_i \ldots CD_n$ , respectively. The quadrilateral block moves with an absolute velocity $V_{qb}$, , which makes an angle $\phi$ with $D_{qb}E$ and an angle $\psi = \left(\frac{\pi}{2} + \beta_{qb} - \theta - \phi - \sum_{j=1}^{n} \alpha_j\right)$ with the skirt BC, as shown in Fig. 1b. It is worth noting that in the presence of soil cohesion, an adhesion factor ($\alpha^a$) is assumed to determine the internal energy dissipation along the skirt surface, which ensures no separation between the skirt and the soil. All the velocities can be computed in terms of $V_0$ following the velocity hodograph, as shown in Fig. 1b.

## 4 ANALYSIS

Various parameters along with the velocity vectors associated with the radial shear zone around the edge of the foundation can be obtained following the collapse mechanism as well as the velocity hodograph. The magnitude of $P_{usk}$ can be obtained by equating the total external work done to the total internal dissipation of energy, which in turn determines the ultimate bearing capacity of the skirted foundation, $q_{usk} = P_{usk}/B_f$. The work done by various external forces and the internal dissipation of energy along the lines of discontinuity can be obtained by following the equations provided in Appendix I and II, respectively. Among the various possible solutions obtained with different input parameters, the least upper-bound value of $P_{usk}$ reveals the target solution. Hence, the objective function (the bearing capacity) is optimized with respect to different variables (geometrical parameters of the failure mechanism) to obtain the minimum value of the bearing capacity and can be expressed as

$$q_{usk} = \frac{P_{usk}}{B_f} = cN_{csk} + 0.5\gamma B_f N_{\gamma sk} \qquad (1)$$

The bearing-capacity factors for the smooth skirts can be expressed as

$$N_{\gamma sk} = -(f_1 + f_2 + f_3 + f_4 + f_5) \qquad (2a)$$

$$N_{csk} = (f_6 + f_7 + f_8 + f_9 + f_{10}) \qquad (2b)$$

where the functions $f_1 - f_{10}$ are defined in Appendix I and II. However, for a detailed formulation of these functions, Chen [29] can be referred to.

Similarly, the bearing-capacity factors for the rough skirts can be expressed as

$$N_{\gamma sk} = -(f_1 + f_2 + f_3 + f_4 + f_5) \qquad (3a)$$

$$N_{csk} = (f_6 + f_7 + f_8 + f_9 + f_{10} + f_{11}) \qquad (3b)$$

where the function $f_{11}$ is defined in Appendix II.

From Eqs. (2) and (3) it can be observed that $N_{\gamma sk}$ is same for the foundation with smooth as well as rough skirts, whereas $N_{csk}$ varies with the roughness of the skirts. The method of superposition is employed to determine the bearing-capacity factor for the skirted foundation i.e., the $c = 0$, $\gamma \neq 0$ condition is considered to determine $N_{\gamma sk}$; whereas $N_{csk}$ is obtained by considering the $c \neq 0$, $\gamma = 0$ condition and hence, in the process, a true upper-bound solution might not be guaranteed. The minimum value of the bearing capacity, $q_{usk}$ is obtained after performing a nonlinear constrained optimization of Eq. (1) with the help of the 'fmincon' solver in MATLAB.

The constraints considered in the optimization process are

a) $\theta + \sum_{j=1}^{n+1} \alpha_j + \alpha_{qb} = \pi$, which is based on the geometry of the failure mechanism.

b) $\alpha_i + \beta_i > \beta_{i+1}$, which ensures a kinematically admissible failure mechanism.

c) $\alpha_i + \beta_i < \pi$, which ensures that all the rigid blocks within the radial shear zone are triangular.

d) $10° < \theta < 85°$, $1° < \alpha_i < 85°$, $10° < \beta_i < 170°$, which are the upper and lower limits of the parameters $\theta$, $\alpha_i$ and $\beta_i$.

e) $V_i > 0$ and $V_{i-1} < V_i$, which ensure that all the velocity vectors are positive and the collapse mechanism is kinematically admissible.

## 5 RESULTS AND DISCUSSION

### 5.1 Smooth and rough skirts

The variation of $N_{csk}$ with $D_f/B_f$ for both smooth and rough skirts is shown in Fig. 2 for different values of $\alpha^a$ and $\phi$. For smooth skirts, there is no energy dissipation along the skirts; whereas in the case of rough skirts the magnitude of $N_{csk}$ depends on the adhesion factor $\alpha^a$, which is varied from 1/3 to 1.0. From Fig. 2 it is clear that the magnitude of $N_{csk}$ increases with an increase in the $D_f/B_f$ ratio for a particular value of $\phi$. It can also be observed that the value of $N_{csk}$ increases as the roughness of the skirts i.e., the adhesion factor ($\alpha^a$), increases. However, for a lower embedment ratio ($D_f/B_f$) the roughness of the skirts has little influence on $N_{csk}$. Hence, it is evident from Fig. 2 that the effectiveness of the skirted foundation increases with an increase in the embedment depth of the skirt.

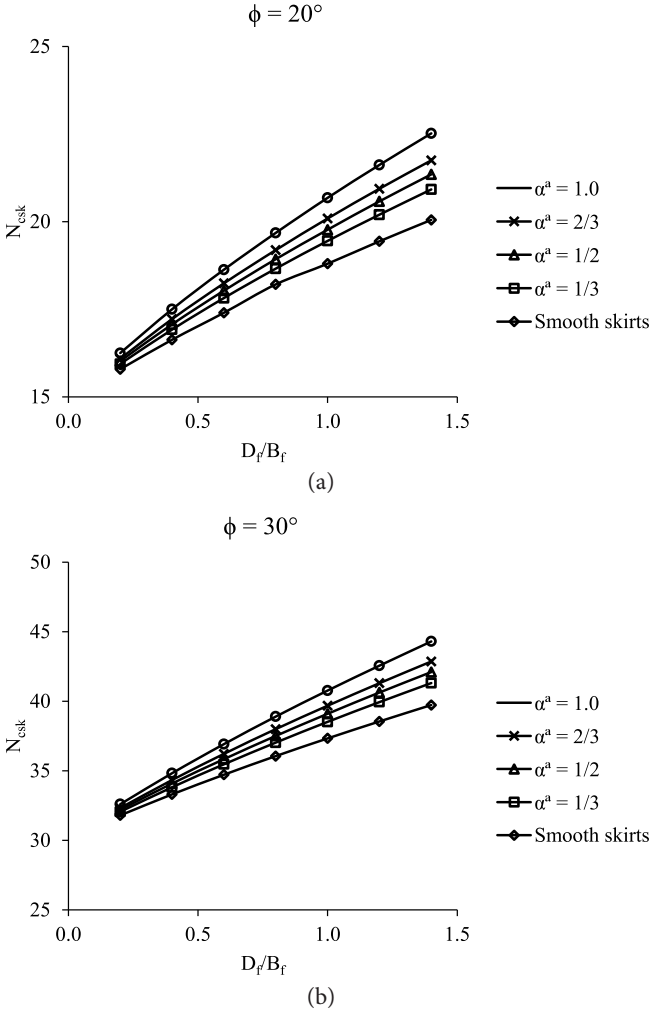


**Figure 2**. (a) Variation of $N_{csk}$ with $D_f/B_f$ with different $\alpha^a$ for (a) $\phi = 20°$, (b) $\phi = 30°$.

The variation of $N_{ysk}$ with $D_f/B_f$ for different values of $\phi$ is shown in Fig. 3. The magnitude of $N_{ysk}$ is found to increase significantly with the $D_f/B_f$ ratio due to an increase in the confinement provided by the skirts. The roughness of the skirts does not affect the bearing-capacity factor $N_{ysk}$ as the internal energy dissipation is considered to be zero ($c = 0$) in the determination of $N_{ysk}$. The rate of increase of $N_{ysk}$ is seen to be more predominant in the case of a higher angle of internal friction, which can be attributed to the larger failure domain developed in the surrounding soil.

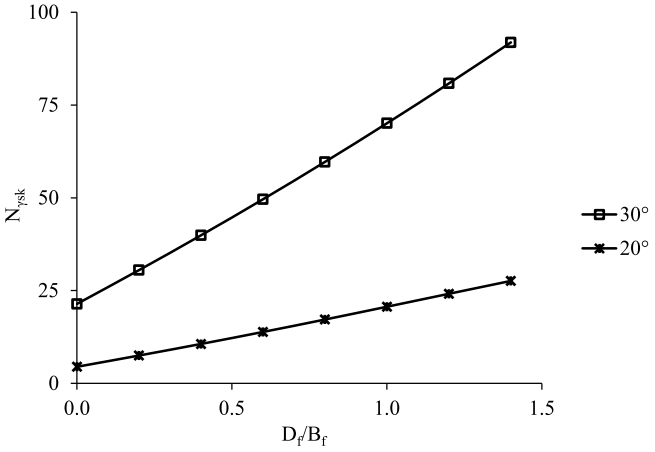


**Figure 3**. Variation of $N_{ysk}$ with $D_f/B_f$ for different values of $\phi$.

### 5.2 Critical failure surface

The critical failure surface obtained from the optimization of the collapse mechanism is shown in Fig. 4 for $\phi = 30°$ and different $D_f/B_f$ ratios. It is clear that the size of the critical failure zone considerably increases with an increase in the $D_f/B_f$ ratio, which in turn causes an increase in the bearing capacity of the skirted foundation. Similarly, the critical failure surface for different values of $\alpha^a$ and $\phi$ is presented in Figs. 5 and 6, respectively. It is clear from Figs. 5 and 6 that the failure zone expands with an increase in $\alpha^a$ and $\phi$, resulting in an enhancement of the bearing capacity with an increasing roughness of the skirts and the angle of internal friction of the surrounding soil.

## 6 COMPARISON

In Table 1 the present values of $N_{csk}$ obtained for smooth skirts with $\phi = 0°$ are compared with those reported by Mana et al. [15], who obtained $N_{csk}$ for the foundation with smooth skirts employing finite-element limit

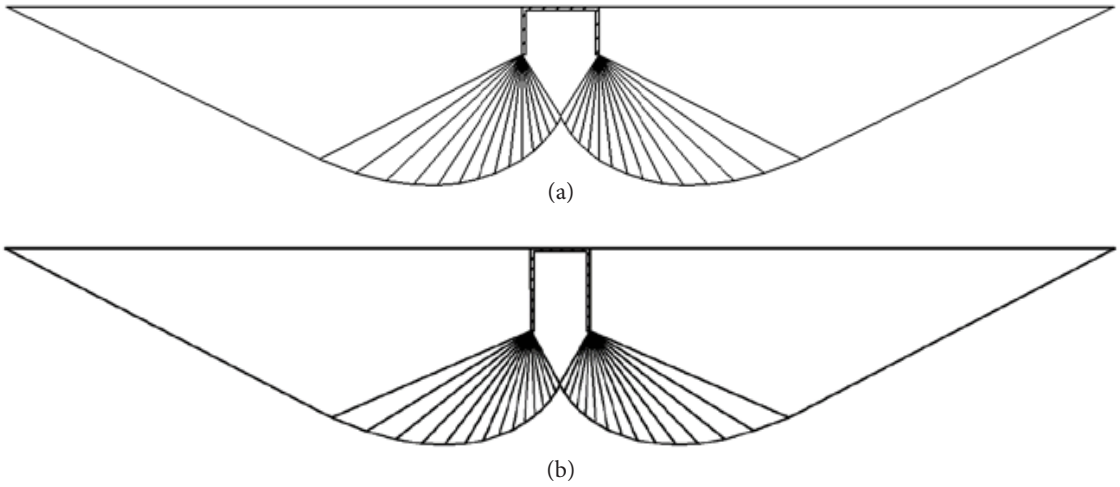


**Figure 4**. Critical collapse surface for $\phi = 30°$ and $\alpha^a = 1.0$ with (a) $D_f/B_f = 0.6$, (b) $D_f/B_f = 1.4$.

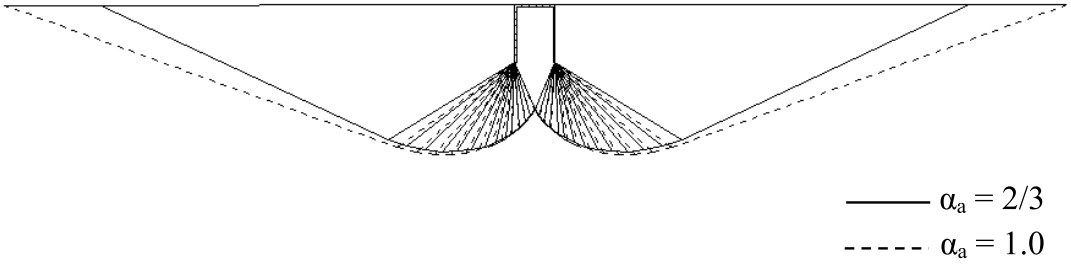


**Figure 5**. Critical collapse surface for $\phi = 30°$and $D_f/B_f = 1.4$ with different $\alpha^a$.

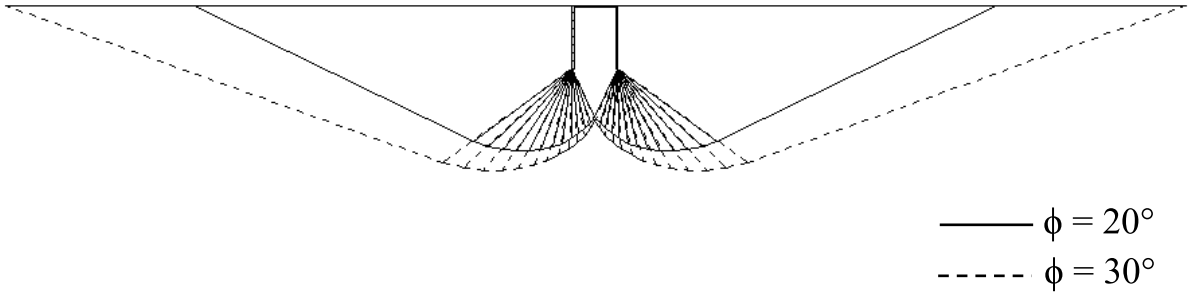


**Figure 6**. Critical collapse surface for $\alpha^a = 1.0$ and $D_f/B_f = 1.4$ with different $\phi$.

analysis. The present results are found to be the lowest, but compare reasonably well with those proposed by Mana et al. [15]. In Table 2, the values of $N_{csk}$ obtained from the present analysis for rough skirts with $\phi = 0°$ are compared with those provided by Yun and Bransby [21] and Mana et al. [14]. The latter determined the bearing-capacity of a skirted strip foundation resting on uniform clay soil ($\phi = 0°$) using the finite-element method. The present analysis predicts a lower value of $N_{csk}$ as compared with the existing values reported in the literature and hence it can be considered as a better solution for the skirted foundation.

In Table 3, the ratio of $N_{ysk}/N_\gamma$ obtained from the present analysis for different magnitudes of the $D_f/B_f$ ratio is compared with the numerical as well as the experimental results reported by Eid [11]. Eid [11] proposed the $N_{ysk}/N_\gamma$ ratio in cohesionless soil through experimental

**Table 1**. Comparison of $N_{csk}$ for smooth skirts with $\phi = 0°$.

| $D_f/B_f$ | Present analysis | Mana et al. [15] |
|---|---|---|
| 0.1 | 5.33 | 5.48 |
| 0.2 | 5.50 | 5.74 |
| 0.3 | 5.63 | 5.92 |
| 0.4 | 5.77 | 6.10 |
| 0.5 | 5.90 | 6.22 |

**Table 2**. Comparison of $N_{csk}$ for rough skirts with $\phi = 0°$.

| $D_f/B_f$ | Present analysis | Yun and Bransby [21] | Mana et al. [14] |
|---|---|---|---|
| 0.00 | 5.14 | 5.20 | 5.22 |
| 0.20 | 5.65 | 6.00 | 6.10 |
| 0.30 | 5.86 | 6.35 | 6.50 |
| 0.50 | 6.23 | 7.00 | 7.25 |
| 0.75 | 6.62 | 7.70 | 8.00 |
| 1.00 | 6.95 | 8.50 | 8.80 |
| 1.20 | 7.19 | 9.00 | - |

**Table3**. Comparison of $N_{ysk}/N_\gamma$ ratio for different $D_f/B_f$.

| $\phi$(°) | $D_f/B_f$ | $N_{ysk}/N_\gamma$ | | |
|---|---|---|---|---|
| | | Present analysis | Eid [11] | |
| | | | Numerical | Experimental |
| 35.0 | 0.5 | 1.87 | 1.5 | - |
| | 1.0 | 2.80 | 1.8 | - |
| | 1.5 | 3.81 | 2.6 | - |
| | 2.0 | 4.88 | 3.2 | - |
| 38.5 | 0.5 | 1.74 | - | 2.10 |
| | 1.0 | 2.52 | - | 3.10 |
| | 1.5 | 3.36 | - | 4.05 |
| | 2.0 | 4.25 | - | 5.50 |
| 40.0 | 0.5 | 1.70 | 1.4 | 1.85 |
| | 1.0 | 2.41 | 2.1 | 2.60 |
| | 1.5 | 3.18 | 2.6 | 3.50 |
| | 2.0 | 4.00 | 3.2 | 4.70 |
| 45.0 | 0.5 | 1.53 | 1.6 | 1.50 |
| | 1.0 | 2.10 | 2.2 | 2.20 |
| | 1.5 | 2.66 | 2.7 | 2.95 |
| | 2.0 | 3.27 | 3.3 | 4.00 |

as well as numerical analyses. Three different values of relative density (44%, 57% and 71%) were considered in the experimental study of Eid [11], which correspond to three different magnitudes of $\phi$ , such as 38.5°, 40° and 45° [30]. It is worth noting that the corresponding value of $\phi$ is selected as the mean value within the range of $\phi$ as proposed by Eid et al. [30]. For lower values of $\phi$, the present values of the $N_{ysk}/N_\gamma$ ratio are seen to be a little higher than those determined from the numerical study of Eid [11], whereas the experimental results of Eid [11] for all values of $\phi$ are the highest.

## 7 CONCLUSIONS

The bearing-capacity factors for a skirted strip foundation are determined using an upper-bound limit analysis for various soil-friction angles and the embedment ratio of the skirts. The magnitude of $N_{csk}$ is found to increase with an increase in the roughness of the skirts. However, for a lower value of the $D_f/B_f$ ratio, the roughness of the skirts has little influence on the $N_{csk}$ values. It was clear that the magnitude of $N_{csk}$ increases with an increase in the $D_f/B_f$ ratio for a particular value of $\phi$. The magnitude of $N_{ysk}$ was found to increase significantly with the$D_f/B_f$ ratio due to an increase in the confinement provided by the skirts. The roughness of the skirts does not affect $N_{ysk}$ as the internal energy dissipation is considered to be zero ($c = 0$) during the calculation of $N_{ysk}$.

## APPENDIX I: EXTERNAL WORK DONE

a) The external work done by the self-weight of the quadrilateral block $ABCD_1$ below the footing (Fig. 1a) can be expressed as,

$$\Delta W_{ABCD_1} = \frac{\gamma B_f^{\,2}}{2}[f_1(\alpha_i, \beta_i, \theta)]V_0 \qquad (4)$$

where,

$f_1 = \frac{\tan\theta}{2} + 2\left(\frac{D_f}{B_f}\right)$

b) The external work done by the self-weight of the $2n$ triangular rigid blocks on either side of the footing can be expressed as,

$$\sum_{j=1}^{2n}[\Delta W]_j = \frac{\gamma B_f^{\,2}}{2}[f_2(\alpha_i, \beta_i, \theta)]V_0 \qquad (5)$$

where,

$$f_2 = \frac{\cos(\theta-\phi)}{2\cos^2\theta\sin(\beta_1-2\phi)}\sum_{i=1}^{n}\left[\frac{\sin\alpha_i\sin\beta_i}{\sin(\alpha_i+\beta_i)}\right.$$

$$\left.\sin\left(\beta_i-\theta-\phi-\sum_{j=1}^{i-1}\alpha_j\right)\prod_{j=1}^{i-1}\frac{\sin^2\beta_j}{\sin^2(\alpha_j+\beta_j)}\frac{\sin(\alpha_j+\beta_j-2\phi)}{\sin(\beta_{j+1}-2\phi)}\right]$$

c) The external work done by the self-weight of the quadrilateral rigid block $BCD_{qb}E$ (Fig. 1a) can be expressed as,

$$\Delta W_{qb} = \frac{\gamma B_f^{\,2}}{2}[f_3(\alpha_i, \beta_i, \theta) + f_4(\alpha_i, \beta_i, \theta) + f_5(\alpha_i, \beta_i, \theta)]V_0 \quad (6)$$

where,

$$f_3 = \left[\frac{cos(\theta-\phi)\,sin\,\alpha_{qb}\,sin\,\beta_{qb}}{2\,cos^2\theta\,sin(\alpha_{qb}+\beta_{qb})\,sin(\beta_1-2\phi)}\right.$$
$$\left.sin\left(\beta_{qb}-\theta-\phi-\sum_{j=1}^{n}\alpha_j\right)\prod_{j=1}^{n}\frac{sin^2\,\beta_j\,sin(\alpha_j+\beta_j-2\phi)}{sin^2(\alpha_j+\beta_j)\,sin(\beta_{j+1}-2\phi)}\right]$$

$$f_4 = \left[\frac{2D_f}{B_f}\frac{cos(\theta-\phi)\,sin\,\beta_{qb}}{cos\,\theta\,sin(\beta_1-2\phi)\,sin(\alpha_{qb}+\beta_{qb})}\right.$$
$$\left.sin\left(\beta_{qb}-\theta-\phi-\sum_{j=1}^{n}\alpha_j\right)\prod_{j=1}^{n}\frac{sin\,\beta_j\,sin(\alpha_j+\beta_j-2\phi)}{sin(\alpha_j+\beta_j)\,sin(\beta_{j+1}-2\phi)}\right]$$

$$f_5 = \left[\frac{2D_f^{\,2}}{B_f^{\,2}}\frac{cos(\theta-\phi)\,sin\left[(\alpha_{qb}+\beta_{qb})-\pi/2\right]}{sin(\beta_1-2\phi)\,sin(\alpha_{qb}+\beta_{qb})}\right.$$
$$\left.\cdot sin\left(\beta_{qb}-\theta-\phi-\sum_{j=1}^{n}\alpha_j\right)\prod_{j=1}^{n}\frac{sin(\alpha_j+\beta_j-2\phi)}{sin(\beta_{j+1}-2\phi)}\right]$$

d) The external work done by the foundation load $P_{usk}$ can be expressed as,

$$\Delta W_f = P_{usk}V_0 \quad (7)$$

## APPENDIX II: INTERNAL DISSIPATION OF ENERGY

Considering the complete failure mechanism, the internal dissipation of energy can be derived as follows

a) The internal dissipation of energy along the line of discontinuity $CD_1$ can be expressed as (Fig. 1a),

$$\Delta IWD_{CD_1} = cB_f[f_6(\alpha_i, \beta_i, \theta)]V_0 \quad (8)$$

where,

$$f_6 = \frac{cos\,\phi\,cos(\beta_1-\theta-\phi)}{cos\,\theta\,cos(\beta_1-2\phi)}$$

b) The internal dissipation of energy along $d_i$ ($i$ = 1, 2, 3…..$n$) can be expressed as,

$$\Delta IWD_d = cB_f[f_7(\alpha_i, \beta_i, \theta)]V_0 \quad (9)$$

where,

$$f_7 = \frac{cos(\theta-\phi)\,cos\,\phi}{cos\theta\,sin(\beta_1-2\phi)}$$
$$\sum_{i=1}^{n}\left[\frac{sin\alpha_i}{sin(\alpha_i+\beta_i)}\prod_{j=1}^{i-1}\frac{sin\,\beta_j}{sin(\alpha_j+\beta_j)}\frac{sin(\alpha_j+\beta_j-2\phi)}{sin(\beta_{j+1}-2\phi)}\right]$$

c) The internal dissipation of energy along $l_i$ ($i$ = 2, 3, 4….$n$) can be expressed as,

$$\Delta IWD_l = cB_f[f_8(\alpha_i, \beta_i, \theta)]V_0 \quad (10)$$

where,

$$f_8 = \frac{cos(\theta-\phi)\,cos\,\phi}{cos\theta\,sin(\beta_1-2\phi)}$$
$$\sum_{i=2}^{n+1}\left[\frac{sin(\beta_{i-1}-\beta_i+\alpha_{i-1})}{sin(\beta_i-2\phi)}\prod_{j=1}^{i-1}\frac{sin\,\beta_j}{sin(\alpha_j+\beta_j)}\prod_{j=1}^{i-2}\frac{sin(\alpha_j+\beta_j-2\phi)}{sin(\beta_{j+1}-2\phi)}\right]$$

d) The internal dissipation of energy along the discontinuity line $D_{qb}E$ for the last quadrilateral block (Fig. 1a) can be expressed as,

$$\Delta IWD_{D_{qb}E} = cB_f[f_9(\alpha_i, \beta_i, \theta) + f_{10}(\alpha_i, \beta_i, \theta)]V_0 \quad (11)$$

where,

$$f_9 = \frac{cos(\theta-\phi)\,cos\,\phi\,sin\,\alpha_{qb}}{cos\theta\,sin(\beta_1-2\phi)\,sin(\alpha_{qb}+\beta_{qb})}$$
$$\prod_{j=1}^{n}\frac{sin\,\beta_j}{sin(\alpha_j+\beta_j)}\frac{sin(\alpha_j+\beta_j-2\phi)}{sin(\beta_{j+1}-2\phi)}$$

$$f_{10} = \frac{2D_f}{B_f}\frac{cos(\theta-\phi)\,cos\,\phi}{sin(\beta_1-2\phi)\,sin(\alpha_{qb}+\beta_{qb})}\prod_{j=1}^{n}\frac{sin(\alpha_j+\beta_j-2\phi)}{sin(\beta_{j+1}-2\phi)}$$

e) The internal dissipation of energy along the skirts i.e., along BC (Fig. 1a), can be expressed as,

$$\Delta IWD_{BC} = cB_f[f_{11}(\alpha_i, \beta_i, \theta)]V_0 \quad (12)$$

where,

$$f_{11} = \alpha^a\frac{D_f}{B_f}\frac{cos(\theta-\phi)}{sin(\beta_1-2\phi)}$$
$$cos\left(\frac{\pi}{2}+\beta_{qb}-\theta-\phi-\sum_{j=1}^{n}\alpha_j\right)\prod_{j=1}^{n}\frac{sin(\alpha_j+\beta_j-2\phi)}{sin(\beta_{j+1}-2\phi)}$$

## REFERENCES


[1] Alemi, M., Maia, R. 2018. Numerical simulation of the flow and local scour process around single and complex bridge piers. International Journal of Civil Engineering 16(5), 475-487. DOI: https://doi.org/10.1007/s40999-016-0137-8

[2] Keawsawasvong, S., Ukritchon, B. 2016. Finite element limit analysis of pullout capacity of planar caissons in clay. Computers and Geotechnics 75, 12-17. DOI: https://doi.org/10.1016/j.compgeo.2016.01.015

[3] Ukritchon, B., Keawsawasvong, S. 2016. Undrained pullout capacity of cylindrical suction caissons by finite element limit analysis. Computers

and Geotechnics 80, 301-311. DOI: https://doi.org/10.1016/j.compgeo.2016.08.019

[4] Ukritchon, B., Wongtoythong, P., Keawsawasvong, S. 2018. New design equation for undrained pullout capacity of suction caissons considering combined effects of caisson aspect ratio, adhesion factor at interface, and linearly increasing strength. Applied Ocean Research 75, 1-14. DOI: https://doi.org/10.1016/j.apor.2018.03.007

[5] Al-Aghbari, M.Y., Dutta, R.K. 2008. Performance of square footing with structural skirt resting on sand. Geomechanics and Geoengineering 3(4), 271–277. DOI: https://doi.org/10.1080/17486020802509393

[6] Al-Aghbari, M.Y., Zein, Y.E. 2004. Bearing capacity of strip foundations with structural skirts. Geotechnical and Geological Engineering 22(1), 43-57. DOI: 10.1023/B:GEGE.0000013997.79473.e0

[7] Azzam, W.R. 2015. Finite element analysis of skirted foundation adjacent to sand slope under earthquake loading. HBRC Journal, 11(2), 231-239. DOI: https://doi.org/10.1016/j.hbrcj.2014.04.001

[8] Bienen, B., Gaudin, C., Cassidy, M.J., Rausch, L., Purwana, O.A., Krisdani, H. 2012. Numerical modelling of a hybrid skirted foundation under combined loading. Computers and Geotechnics 45, 127-139. DOI: https://doi.org/10.1016/j.compgeo.2012.05.009

[9] Bransby, M.F., Randolph, M.F. 1998. Combined loading of skirted foundations. Géotechnique 48(5), 637–655. DOI: https://doi.org/10.1680/geot.1998.48.5.637

[10] Bransby, M.F., Randolph, M.F. 1999. The effect of embedment depth on the undrained response of skirted foundations to combined loading. Soils and Foundations 39(4), 19–33. DOI: https://doi.org/10.3208/sandf.39.4_19

[11] Eid, H.T. 2013. Bearing capacity and settlement of skirted shallow foundations on sand. International Journal of Geomechanics 13(5), 645–652. DOI: https://doi.org/10.1061/(ASCE)GM.1943-5622.0000237

[12] Gourvenec, S. 2008. Effect of embedment on the undrained capacity of shallow foundations under general loading. Géotechnique 58(3), 177–185. DOI: https://doi.org/10.1680/geot.2008.58.3.177

[13] Gourvenec. S., Barnett, S. 2011. Undrained failure envelope for skirted foundations under general loading. Géotechnique 61(3), 263–270. DOI: https://doi.org/10.1680/geot.9.T.027

[14] Mana, D.S.K., Gourvenec, S.M., Randolph, M.F. 2010. A numerical study of the vertical bearing capacity of skirted foundations. Proceeding of 2nd International Symposium on Frontiers in Offshore Geotechnics (ISFOG), Perth, Australia, pp. 433–438.

[15] Mana, D.S.K., Gourvenec, S., Martin, C.M. 2013. Critical skirt spacing for shallow foundations under general loading. Journal of Geotechnical and Geoenvironmental Engineering 139(9), 1554-1566. DOI: https://doi.org/10.1061/(ASCE)GT.1943-5606.0000882

[16] Martin, C.M. 2001. Vertical bearing capacity of skirted circular foundations on Tresca soil. Proceeding of 15th International Conference on Soil Mechanics and Geotechnical Engineering, Istanbul, Turkey, 1, pp. 743–746.

[17] Pal, A., Ghosh, P., Majumder, M. 2017. Interaction effect of two closely spaced skirted strip foundations in cohesionless soil using upper-bound limit analysis. International Journal of Geomechanics 17(2), 06016022. DOI: https://doi.org/10.1061/(ASCE)GM.1943-5622.0000755

[18] Punrattanasin, P., Izawa, J., Kusakabe, O., Murata, O., Koda, M., Nishioka, H. 2003. The behavior of sheet pile foundations on sand. Proceeding of British Geotechnical Association (BGA) International Conference on Foundations, T. A. Newson, ed., MPG Books, Bodmin, U.K., pp. 723–732.

[19] Punrattanasin, P., Gasaluck, W., Muktabhant, C., Angsuwotai, P., Patjanasuntorn, A. 2009. The effect of sheet pile length on the capacity of sheet pile foundation. Proceeding of 17th International Conference on Soil Mechanics and Geotechnical Engineering, Millpress Science Publishers, Rotterdam, Netherlands, 1, pp. 598–601.

[20] Villalobos, F., Byrne, B.W., Houlsby, G.T., Martin, C.M. 2003. Bearing capacity tests of scale suction caisson footings on sand: Experimental data. Data Rep. FOT005/1, Department of Engineering Science, University of Oxford, Oxford, U.K.

[21] Yun, G., Bransby, M.F. 2007. The undrained vertical bearing capacity of skirted foundations. Soils and Foundations 47(3), 493–505. DOI: https://doi.org/10.3208/sandf.47.493

[22] Ghosh, P. 2008. Upper bound solutions of bearing capacity of strip footing by pseudo-dynamic approach. Acta Geotechnica 3(2), 115 -123. DOI: https://doi.org/10.1007/s11440-008-0058-z

[23] Kaya, N., Ornek, M. 2013. Experimental numerical studies of T-shaped footings. Acta Geotechnica Slovenica 10(1), 43-58.

[24] Shukla, R.P., Jakka, R.S. 2017. Critical setback distance for a footing resting on slopes. Acta Geotechnica Slovenica 14(2), 19-31.

[25] Ukritchon, B., Keawsawasvong, S. 2016. A practical method for the optimal design of continuous foot-

ing using ant-colony optimization. Acta Geotechnica Slovenica 13(2), 45-55.

[26] Ukritchon, B., Keawsawasvong, S. 2017. Unsafe error in conventional shape factor for shallow circular foundations in normally consolidated clays. Journal of Geotechnical and Geoenvironmental Engineering 143(6), 02817001. DOI: https://doi.org/10.1061/(ASCE)GT.1943-5606.0001670

[27] Ukritchon, B., Keawsawasvong, S. 2018. Lower bound limit analysis of an anisotropic undrained strength criterion using second-order cone programming. International Journal for Numerical and Analytical Methods in Geomechanics 42(8), 1016-1033. DOI: https://doi.org/10.1002/nag.2781

[28] Ukritchon, B., Yoang, S., Keawsawasvong, S. 2018. Bearing capacity of shallow foundations in clay with linear increase in strength and adhesion factor. Marine Georesources and Geotechnology 36(4), 438-451. DOI: 10.1080/1064119X.2017.1326991

[29] Chen, W.F. 1975. Limit analysis and soil plasticity. Elsevier, Amsterdam, Netherland.

[30] Eid, H.T., Alansari, O.A., Odeh, A.M., Nasr, M.N., Sadek, H.A. 2009. Comparative study on the behavior of square foundations resting on confined sand. Canadian Geotechnical Journal 46(4), 438–453. DOI: https://doi.org/10.1139/T08-134